Supporting Information

“Cage-Confinement” Controlled Dimensionality Conversion of Bi_2O_2Se Crystals towards High-Performance Phototransistors

Kaiyi Zhang,[a] Fang Wang[a], Lei Zheng,[a] Junqing Wei[a], Yongxu Hu,[b] Yangyang Xie,[a] Hongling Guo,[a] Fengpu Zhang[a], Xin Lin[a], Zewen Li[a], Tianling Ren[c], Zhitang Song[d] and Kailiang Zhang*[a]*

[a], Tianjin Key Laboratory of Film Electronic and Communication Devices, School of Integrated Circuit Science and Engineering, Tianjin University of Technology, Tianjin 300384, China.

[b] Key Laboratory of Organic Integrated Circuits, Ministry of Education, Institute of Molecular Aggregation Science, Department of Chemistry, School of Science, Tianjin University, Tianjin 300072, China

[c] Beijing National Research Center for Information Science and Technology Institute of Microelectronics, Tsinghua University, Beijing 100084, China

[d] Shanghai Institute of Microsystem and Information Technology, Chinese Academy of Sciences, Shanghai 200050, China.

*Corresponding authors.

E-mail address: leizheng@tju.edu.cn (Lei Zheng),

kailiang_zhang2007@163.com (Kailiang Zhang)

Keywords: Bi_2O_2Se crystal, controllable dimension, “cage-confinement” growth, van der Waals integrated technique, photodetectors

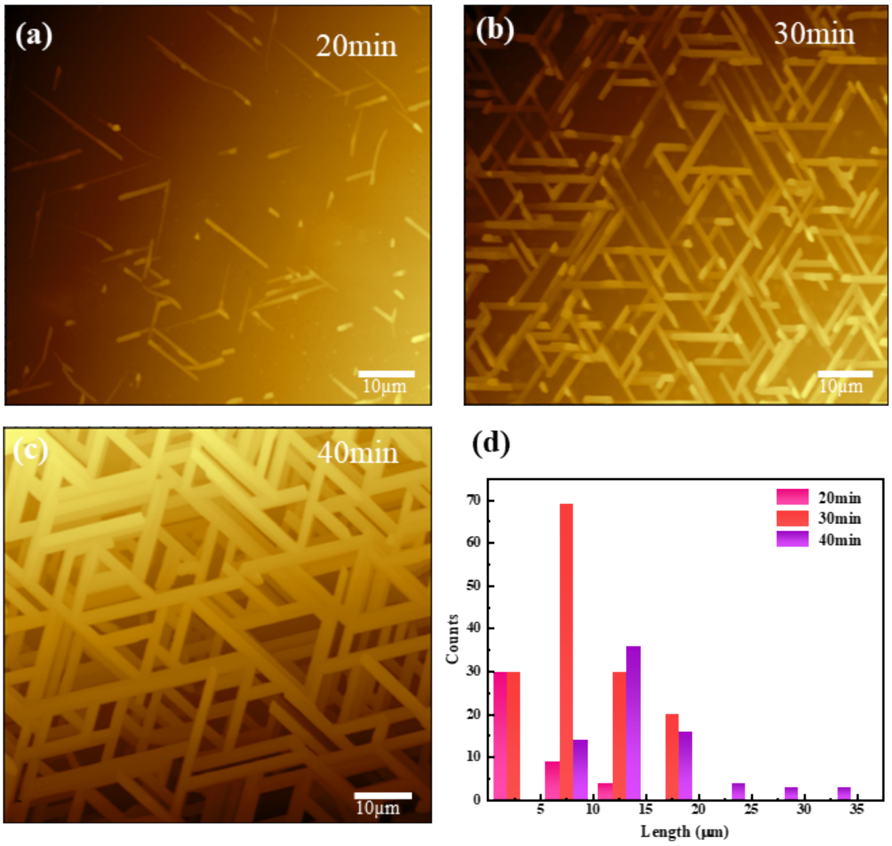

Fig. S1. AFM images of Bi_2O_2Se nanowires at different growth time. a) 20 min sample. b) 30 min sample. c) 40 min sample. d) Statistical diagram of Bi_2O_2Se nanowire lengths.

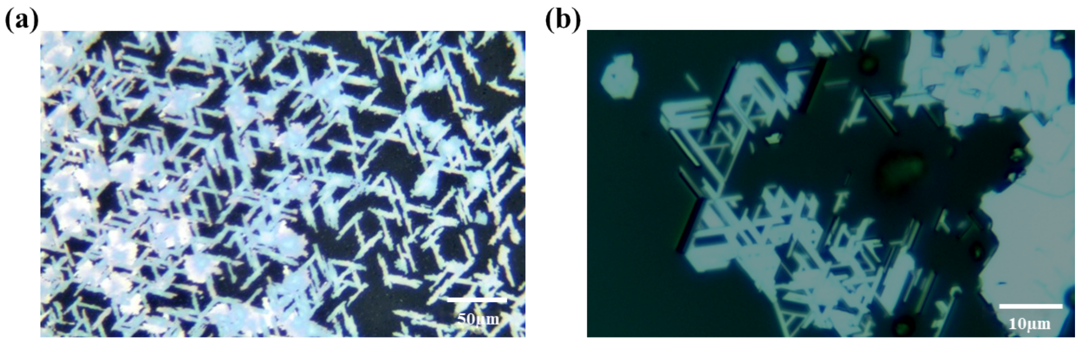

Fig. S2. OM images of Bi_2O_2Se crystals during the process of dimensional transformation (from 1D crystalline nanowires to 2D nanosheets). a) < 500 µm Active area with flow rate of ≈ 100 sccm. b) > 500 µm Active area with flow rate of ≈ 50 sccm.

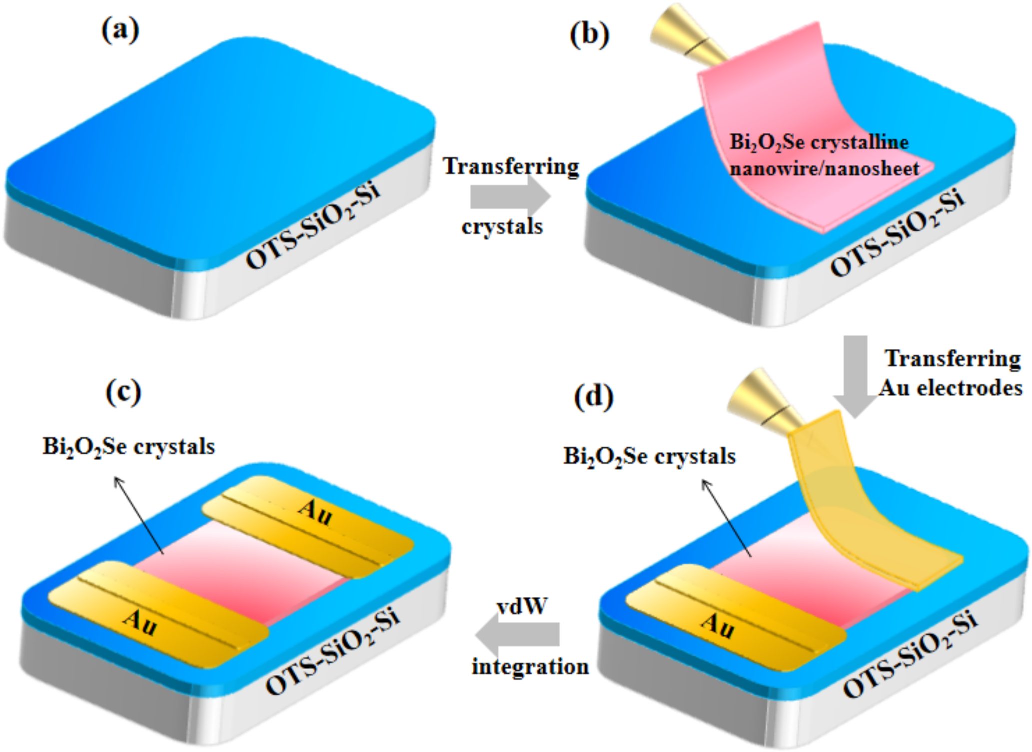

Fig. S3. Schematic illustration of the fabrication processes of Bi_2O_2Se-based FET. a) Incorporation of an OTS monolayer on the SiO_2 substrate. b) Mechanically transferring the Bi_2O_2Se single crystals with the help of probe. c) Stamping the source/drain electrodes onto the Bi_2O_2Se crystals with the help of probe. d) Schematic illustration of a bottom-gate-top-contact Bi_2O_2Se-based FET.

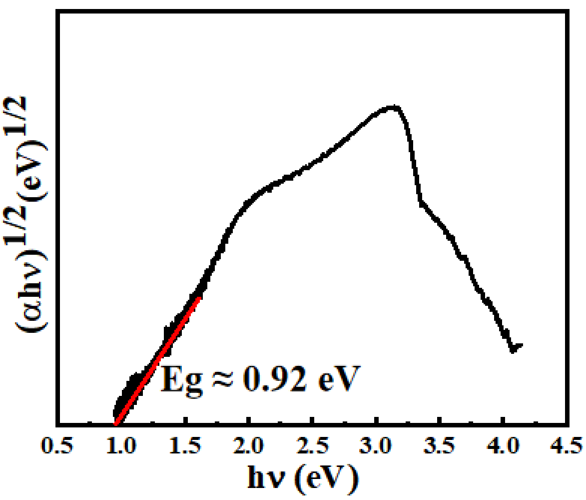

Fig. S4. Approximate value of Eg is calculated by a relationship known as the Tauc plot.

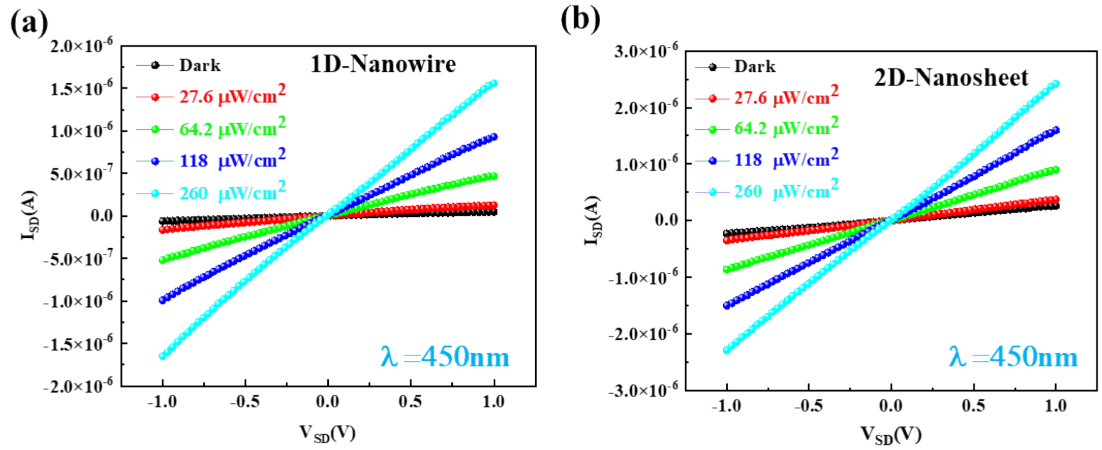

Fig. S5. (a, b) The I_{SD} output curves of 1D and 2D Bi_2O_2Se-based phototransistors under different light power densities conditions (measured at V_G = 60 V and V_{SD} = 1 V)

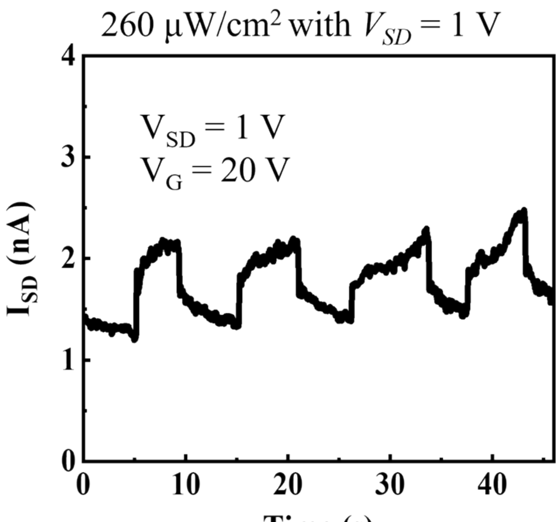

Fig. S6. Time-dependent photo-switching behaviors of Bi_2O_2Se nanoplate photodetector under the 450 nm laser illumination, P = 260 mW/cm^2, bias voltage V_{SD}= 1 V and gate voltage V_G = 20V..

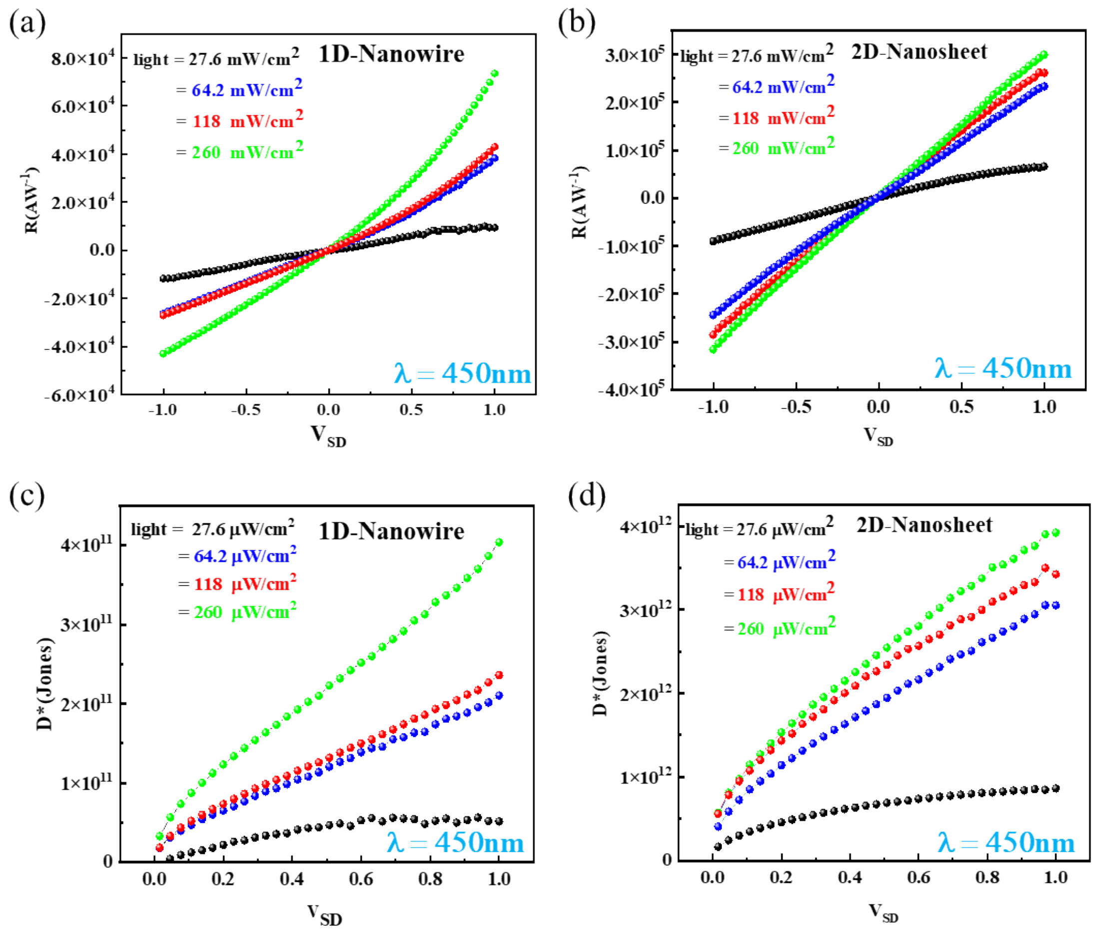

Fig. S7. (a, b) The *R* of Bi_2O_2Se nanowire/nanosheet devices at different light intensity levels, respectively. (c, d) The *D** of Bi_2O_2Se nanowire/nanosheet devices at different light intensity levels, respectively.

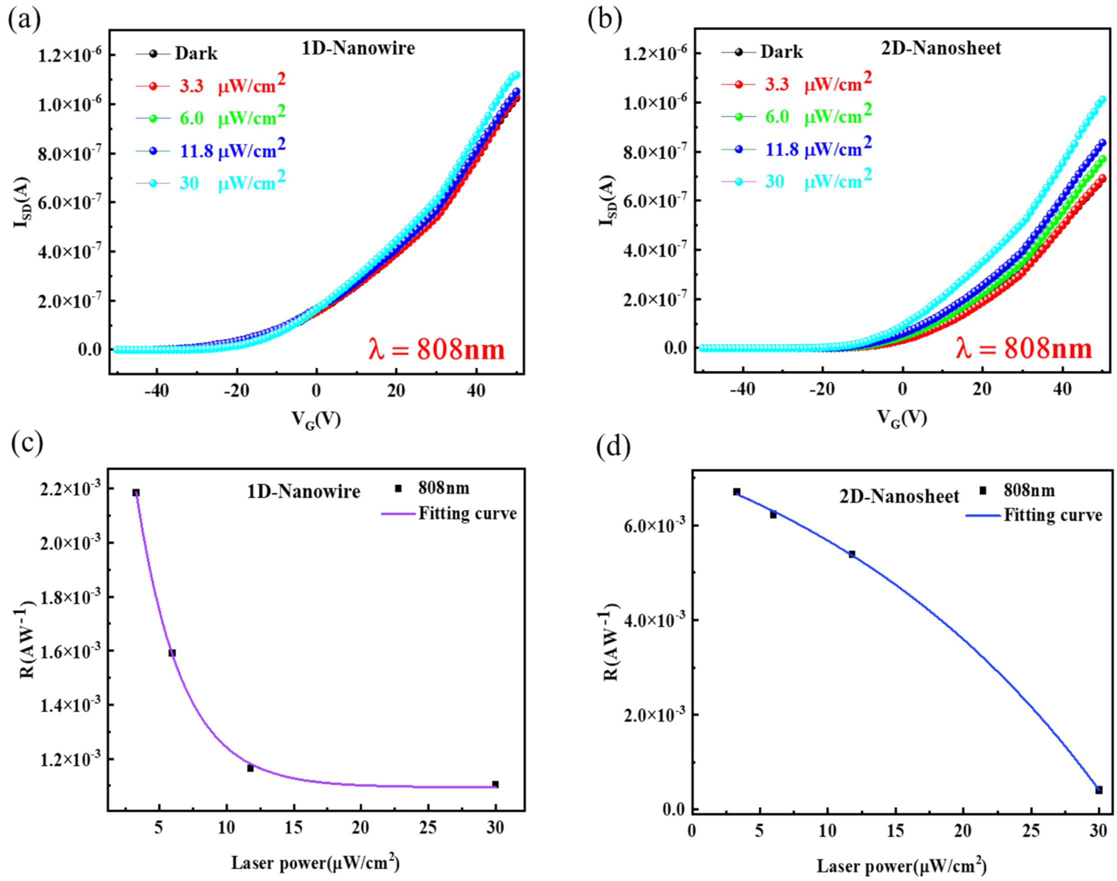

Fig. S8. (a, b) The I_{SD} transfer curves of 1D and 2D Bi_2O_2Se-based phototransistors under different light power densities conditions (measured at V_G = 60 V and V_{SD} = 1 V). (c, d) The R of Bi_2O_2Se 1D/2D devices at different light intensity levels, respectively.

Table S1. Comparison of the responsivity of present Bi_2O_2Se-based photodetectors.

Semiconductor	λ （nm）	Responsivity (A/W)	Ref.
Bi_2O_2Se nanosheet	360	75.14	[1]
Bi_2O_2Se nanosheet	360	108696	[2]
Bi_2O_2Se nanosheet	365	2.068	[3]
Bi_2O_2Se nanoplate	400	523	[4]
Bi_2O_2Se nanosheet	405	45134	[5]
Bi_2O_2Se nanosheet	405	43	[6]
Bi_2O_2Se nanosheet	405	50055	[2]
Bi_2O_2Se nanosheet	500	1.2	[7]
Bi_2O_2Se nanosheet	500	193	[7]
Bi_2O_2Se film	520	6.1	[8]
Bi_2O_2Se nanosheet	532	3×10^3	[9]
Bi_2O_2Se nanosheet	532	2×10^3	[10]
Bi_2O_2Se nanosheet	532	3.5×10^4	[11]
Bi_2O_2Se nanosheet	532	45800	[12]
Bi_2O_2Se nanosheet	532	60	[13]
Bi_2O_2Se nanosheet	532	842.91	[14]
Bi_2O_2Se nanosheet	532	25505	[2]
Bi_2O_2Se nanoribbon	590	9.2×10^6	[15]
Bi_2O_2Se nanosheet	635	44	[6]
Bi_2O_2Se nanosheet	640	9.1	[16]
Bi_2O_2Se film	640	3.8×10^6	[17]
Bi_2O_2Se nanosheet	650	3.94	[3]
Bi_2O_2Se nanosheet	660	22100	[9]
Bi_2O_2Se nanosheet	808	6.5	[11]
Bi_2O_2Se nanosheet	808	843.5	[2]
Bi_2O_2Se nanowire	808	722.2	[19]

Semiconductor	λ （nm）	Responsivities (A/W)	Ref.
Bi_2O_2Se nanosheet	900	101	[18]
Bi_2O_2Se nanosheet	940	300	[21]
Bi_2O_2Se nanosheet	980	0.053	[3]
Bi_2O_2Se nanosheet	1200	65	[22]
Bi_2O_2Se nanosheet	1260	3.5	[07]
Bi_2O_2Se nanosheet	1310	118	[2]
Bi_2O_2Se nanosheet	1550	22.12	[2]
Bi_2O_2Se nanosheet	1550	58	[21]
Bi_2O_2Se nanowire	450	3×10^5	This work
Bi_2O_2Se nanosheet	450	7.4×10^4	This work

REFERENCES

1 M.-Q. Li, L.-Y. Dang, G.-G. Wang, F. Li, M. Han, Z.-P. Wu, G.-Z. Li, Z. Liu, J.-C. Han, Bismuth Oxychalcogenide Nanosheet: Facile Synthesis, Characterization, and Photodetector Application, *Adv. Mater. Technol.,* 2020, **5**(7), 2000180.

2 T. Tong, Y. Chen, S. Qin, W. Li, J. Zhang, C. Zhu, C. Zhang, X. Yuan, X. Chen, Z. Nie, X. Wang, W. Hu, F. Wang, W. Liu, P. Wang, X. Wang, R. Zhang, Y. Xu, Sensitive and Ultrabroadband Phototransistor Based on Two-Dimensional Bi_2O_2Se Nanosheets, *Adv. Funct. Mater.,* 2019, **29**(50), 1905806.

3 X. Xue, C. Ling, H. Ji, J. Wang, C. Wang, H. Lu, W. Liu, Self-Powered and Broadband Bismuth Oxyselenide/p-Silicon Heterojunction Photodetectors with Low Dark Current and Fast Response, *ACS Appl. Mater. Interfaces,* 2023, **15**(4), 5411-5419.

4 H. Wang, S. Zhang, X. Wu, H. Luo, J. Liu, Z. Mu, R. Li, G. Yuan, Y. Liang, J. Tan, Y. Ren, W. Lei, Bi_2O_2Se Nanoplates for Broadband Photodetector and Full-Color Imaging Applications, *Nano Res.,* 2023, **16**(5), 7638-7645.

5 M. Kang, H. Chai, H. B. Jeong, C. Park, I. Jung, E. Park, M. M. Çiçek, I. Lee, B. Bae, E. Durgun, J. Y. Kwak, S. Song, S. Choi, H. Y. Jeong, K. Kang, Low-Temperature and High-Quality Growth of Bi_2O_2Se Layered Semiconductors Via Cracking Metal-Organic Chemical Vapor Deposition, *ACS Nano,* 2021, **15**(5), 8715-8723.

6 L. Tao, S. Li, B. Yao, M. Xia, W. Gao, Y. Yang, X. Wang, N. Huo, Raman Anisotropy and Polarization-Sensitive Photodetection in 2D Bi_2O_2Se - WSe_2 Heterostructure, *ACS Omega,* 2021, **6**(50), 34763-34770.

7 J. Han, C. Fang, M. Yu, J. Cao, K. Huang, A High-Performance Schottky Photodiode with Asymmetric Metal Contacts Constructed on 2D Bi_2O_2Se, *Adv. Electron. Mater.,* 2022, **8**(7), 2100987.

8 X. Pang, Y. Zhao, X. Gao, G. Wang, H. Sun, J. Yin, J. Zhu, Two-Step Colloidal Synthesis of Micron-Scale Bi_2O_2Se Nanosheets and Their Electrostatic Assembly for Thin-Film Photodetectors with Fast Response, *Chin. Chem. Lett.,* 2021, **32**(10), 3099-3104.

9 U. Khan, Y. Luo, L. Tang, C. Teng, J. Liu, B. Liu, H.-M. Cheng, Controlled Vapor - Solid Deposition of Millimeter - Size Single Crystal 2D Bi_2O_2Se for High-Performance Phototransistors, *Adv. Funct. Mater.,* 2019, **29**(14), 1807979.

10 J. Wu, Y. Liu, Z. Tan, C. Tan, J. Yin, T. Li, T. Tu, H. Peng, Chemical Patterning of High-Mobility Semiconducting 2D Bi_2O_2Se Crystals for Integrated Optoelectronic Devices, *Adv. Mater.,* 2017, **29**(44), 1704060.

11 Q. Fu, C. Zhu, X. Zhao, X. Wang, A. Chaturvedi, C. Zhu, X. Wang, Q. Zeng, J. Zhou, F. Liu, B. K. Tay, H. Zhang, S. J. Pennycook, Z. Liu, Ultrasensitive 2D Bi_2O_2Se Phototransistors on Silicon Substrates, *Adv. Mater.,* 2019, **31**(1), 1804945.

12 D. Li, X. Han, G. Xu, X. Lui, X. Zhao, G. Li, H. Hao, J. Dong, H. Liu, J. Xing, Bi_2O_2Se Photoconductive Detector with Low Power Consumption and High Sensitivity, *Acta. Physica. Sinica.,* 2020, **69**(24), 248502.

13 X. Yang, Q. Zhang, Y. Song, Y. Fan, Y. He, Z. Zhu, Z. Bai, Q. Luo, G. Wang, G. Peng, M. Zhu, S. Qin, K. Novoselov, K. High Mobility Two-Dimensional Bismuth

Oxyselenide Single Crystals with Large Grain Size Grown by Reverse-Flow Chemical Vapor Deposition, *ACS Appl. Mater. Interfaces,* 2021, **13**(41), 49153-49162.

14 L. Dang, M. Liu, G. Wang, D. Zhao, J. Han, J. Zhu, Z. Liu, Organic Ion Template - Guided Solution Growth of Ultrathin Bismuth Oxyselenide with Tunable Electronic Properties for Optoelectronic Applications, *Adv. Funct. Mater.,* 2022, **32**(31), 2201020.

15 U. Khan, L. Tang, B. Ding, Y. Luo, S. Feng, W. Chen, M. J. Khan, B. Liu, H. M. Cheng, Catalyst - Free Growth of Atomically Thin Bi_2O_2Se Nanoribbons for High - Performance Electronics and Optoelectronics, *Adv. Funct. Mater.,* 2021, **31**(31) 2101170.

16 Y. Song, Z. Li, H. Li, S. Tang, M. Jiang, Highly Efficient Broadband Photodetectors Based on Lithography-Free Au/Bi_2O_2Se/Au Heterostructures, *Nanoscale,* 2019, **11**(43), 20707-20714.

17 C. Hong, Y. Tao, A. Nie, M. Zhang, N. Wang, R. Li, J. Huang, Y. Huang, X. Ren, Y. Cheng, X. Liu, Inclined Ultrathin Bi_2O_2Se Films: a Building Block for Functional Van Der Waals Heterostructures, *ACS Nano*, 2020, **14**(12), 16803-16812.

18 J. Li, Z. Wang, Y. Wen, J. Chu, L. Yin, R. Cheng, L. Lei, P. He, C. Jiang, L. Feng, J. He, High - Performance Near - Infrared Photodetector Based on Ultrathin Bi_2O_2Se Nanosheets, *Adv. Funct. Mater.,* 2018, **28**(10), 1706437.

19 H. Yang, W. Chen, X. Zheng, D. Yang, Y. Hu, X. Zhang, X. Ye, Y. Zhang, T. Jiang, G. Peng, X. Zhang, R. Zhang, C. Deng, S. Qin, Near-Infrared Photoelectric Properties of Multilayer Bi_2O_2Se Nanofilms, *Nanoscale Res. Lett.* 2019, **14**, 371.

20 J. Li, Z. Wang, J. Chu, Z. Cheng, P. He, J. Wang, L. Yin, R. Cheng, N, Li, Y. Wen, J. He, Oriented Layered Bi_2O_2Se Nanowire Arrays for Ultrasensitive Photodetectors, *Appl. Phys. Lett.* 2019, **114**(15), 151104.

21 Y. Chen, W. Ma, C. Tan, M. Luo, W. Zhou, N. Yao, H. Wang, L. Zhang, T. Xu, T. Tong, Y. Zhou, Y. Xu, C. Yu, C. Shan, H. Peng, F. Yue, P. Wang, Z. Huang, W. Hu, Broadband Bi_2O_2Se Photodetectors from Infrared to Terahertz, *Adv. Funct. Mater.,* 2021, **31**(14), 2009554.

22 J. Yin, Z. Tan, H. Hong, J. Wu, H. Yuan, Y. Liu, C. Chen, C. Tan, F. Yao, T. Li, Y. Chen, Z. Liu, K. Liu, H. Peng, Ultrafast and Highly Sensitive Infrared Photodetectors Based on Two-Dimensional Oxyselenide Crystals, *Nat. Commun.,* 2018, **9**(1), 3311.